

## Supporting Information for

# The *In-situ* Shape-controlled Synthesis and Structure-activity Relationship of Pd Nanocrystal Catalysts Supported on Layered Double Hydroxide

Qiang Zhang,<sup>a</sup> Jing Xu,<sup>a</sup> Dongpeng Yan,<sup>a</sup> Shuangde Li,<sup>a</sup> Jun Lu<sup>\*a</sup>, Xingzhong Cao,<sup>b</sup> and Baoyi Wang<sup>b</sup>

<sup>a</sup> *State Key Laboratory of Chemical Resource Engineering, Beijing University of Chemical Technology, P. Box 98 Beisanhuan East Road 15, Beijing, 100029, P. R. China*

<sup>b</sup> *Institute of High Energy Physics, Chinese Academy of Sciences, Beijing 100049, P. R. China*

\* Corresponding author. E-mail: [lujun@mail.buct.edu.cn](mailto:lujun@mail.buct.edu.cn)

Fax: +86-10-64425385; Tel: +86-10-64412131

## 1. Characterization of materials:

Fourier transform infrared (FT-IR) spectra was recorded in the range 4000 to 400  $\text{cm}^{-1}$  with 2  $\text{cm}^{-1}$  resolution on a Bruker Vector-22 Fourier transform spectrometer using the KBr pellet technique (1 mg of sample in 100 mg of KBr). UV-vis/Diffuse Reflectance spectra for samples was recorded on a UV-vis spectrophotometer (UV-3100, Shimadzu, Japan).  $\text{BaSO}_4$  was used as a reflectance standard in a UV-vis diffuse reflectance experiment. The surface electronic states were analyzed by X-ray photoelectron spectroscopy (XPS) measurement, which was performed using a Perkin-Elmer PHI-5702 X-ray photoelectron spectrometer. X-ray source was a Mg standard anode (1253.6 eV) at 12 kV and 300 W.

## 2. FT-IR spectra

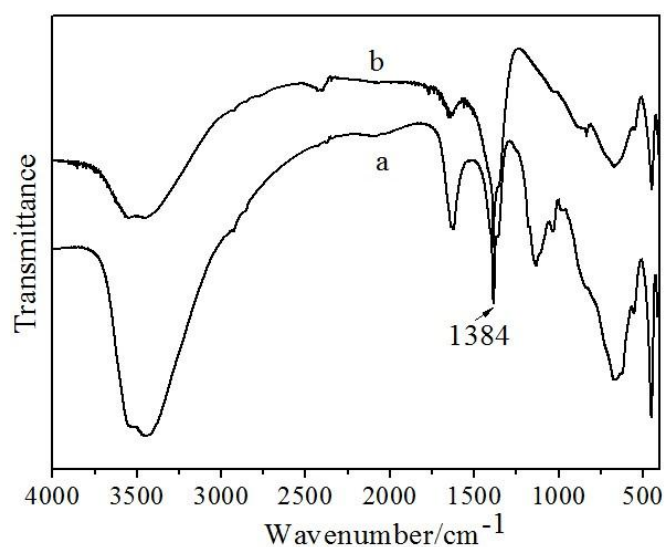


**Figure S1.** FT-IR spectra of (a)  $\text{NO}_3^-$ -LDH and (b)  $\text{PdCl}_4^{2-}$ -LDH.

Figure S1 shows the FT-IR spectrums of  $\text{NO}_3^-$ -LDH and  $\text{PdCl}_4^{2-}$ -LDH samples in the region 400–4000  $\text{cm}^{-1}$ . A strong and broad absorption band centered at  $\sim 3448 \text{ cm}^{-1}$  in the two samples can be identified as the hydroxyl stretching band, arising from metal hydroxyl groups, hydrogen-bonded interlayer water molecules<sup>1</sup>. The absorption band owing to the hydroxyl deformation mode of water,

$\delta(\text{H}_2\text{O})$ , is recorded at around  $1600\text{ cm}^{-1}$ . Bands observed in the range  $500 - 800\text{ cm}^{-1}$  are mainly due to M–O, M–O–M, and O–M–O lattice vibrations. The absorption band attributed to the  $\nu_3$  (asymmetric stretching) mode of  $\text{NO}_3^-$  can also be observed at  $\sim 1384\text{ cm}^{-1}$  in  $\text{PdCl}_4^{2-}$ -LDH, suggesting that  $\text{NO}_3^-$  is not fully exchanged. The characteristic absorption peak of  $\text{CO}_3^{2-}$  does not exist in the FI-IR spectra, which can explain that the size reduction of  $d_{(003)}$  for  $\text{PdCl}_4^{2-}$ -LDH sample is due to the intercalation of the  $\text{PdCl}_4^{2-}$  rather than  $\text{CO}_3^{2-}$ , suggesting that  $\text{PdCl}_4^{2-}$  and  $\text{NO}_3^-$  are co-existed in the LDH interlayer.

### 3. UV-vis/diffuse reflectance spectroscopy

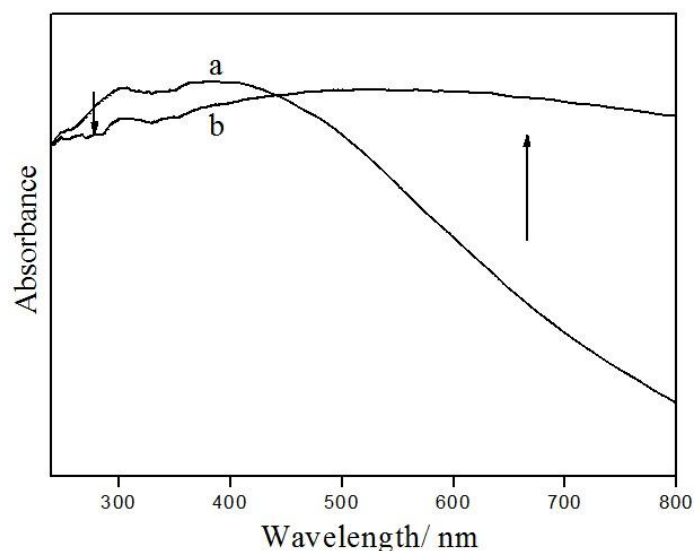


**Figure S2.** UV-vis/diffuse reflectance spectra of (a)  $\text{PdCl}_4^{2-}$ -LDH and (b) Pd-CUs/LDH.

The appearance of LDH-supported Pd NCs was determined by UV-vis/diffuse reflectance spectra. The peak at 280 nm attributed to  $\text{PdCl}_4^{2-}$  disappears after the reduction reaction, and the absorption in the visible region increases,<sup>2</sup> indicating that the Pd NCs are formed.

### 4. The lattice parameters of samples

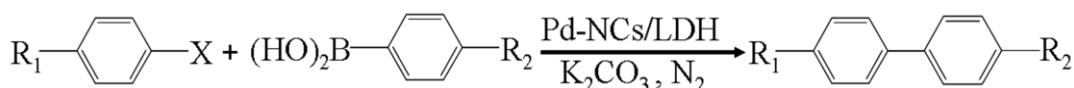
**Table S1.** The lattice parameters of  $\text{NO}_3^-$ -LDH,  $\text{PdCl}_4^{2-}$ -LDH and Pd-CUs/LDH.

LDH	$\text{NO}_3^-$ -LDH	$\text{PdCl}_4^{2-}$ -LDH	Pd-CUs/LDH
-----	----------------------	---------------------------	------------

$d_{003}/\text{nm}$	0.841	0.792	0.762
$d_{006}/\text{nm}$	0.432	0.403	0.379
$d_{009}/\text{nm}$	0.255	0.256	–
$d_{110}/\text{nm}$	0.152	0.152	0.152
$a/\text{nm}$	0.304	0.304	0.304
$c/\text{nm}$	2.523	2.376	2.286

## 5. Suzuki cross-coupling reactions catalyzed by Pd-NCs/LDH catalysts

**Table S2.** The Suzuki cross-coupling reactions catalyzed by different Pd-NCs/LDH catalysts.



Entry	X	R <sub>1</sub>	R <sub>2</sub>	Time/h	Conv/%	Yield/% <sup>d</sup>
1	I	H	Me	4	95 <sup>a</sup>	90 <sup>a</sup>
					92 <sup>b</sup>	88 <sup>b</sup>
					85 <sup>c</sup>	81 <sup>c</sup>
2	I	NO <sub>2</sub>	H	4	99 <sup>a</sup>	98 <sup>a</sup>
					97 <sup>b</sup>	95 <sup>b</sup>
					84 <sup>c</sup>	78 <sup>c</sup>
3	I	NO <sub>2</sub>	OMe	4	97 <sup>a</sup>	95 <sup>a</sup>
					92 <sup>b</sup>	89 <sup>b</sup>
					89 <sup>c</sup>	87 <sup>c</sup>
4	I	OMe	H	4	90 <sup>a</sup>	84 <sup>a</sup>
					83 <sup>b</sup>	76 <sup>b</sup>
					78 <sup>c</sup>	69 <sup>c</sup>
5	Br	H	Me	10	92 <sup>a</sup>	90 <sup>a</sup>
					87 <sup>b</sup>	82 <sup>b</sup>
					80 <sup>c</sup>	75 <sup>c</sup>
6	Br	NO <sub>2</sub>	H	10	97 <sup>a</sup>	92 <sup>a</sup>
					93 <sup>b</sup>	85 <sup>b</sup>
					82 <sup>c</sup>	72 <sup>c</sup>
7	Br	OMe	H	10	83 <sup>a</sup>	80 <sup>a</sup>
					75 <sup>b</sup>	71 <sup>b</sup>
					62 <sup>c</sup>	56 <sup>c</sup>
8	Cl	NO <sub>2</sub>	H	24	82 <sup>a</sup>	76 <sup>a</sup>
					71 <sup>b</sup>	67 <sup>b</sup>
					64 <sup>c</sup>	56 <sup>c</sup>
9	Cl	Me	H	24	73 <sup>a</sup>	63 <sup>a</sup>
					62 <sup>b</sup>	56 <sup>b</sup>
					54 <sup>c</sup>	45 <sup>c</sup>

*Reaction conditions:* Aryl halide (1.0 mmol); arylboronic acid (1.2 mmol); K<sub>2</sub>CO<sub>3</sub> (2.4 mmol);

Pd-NCs/LDH (80 mg, 2 mol%); ethanol : water = 4 : 1(10ml); 75°C; N<sub>2</sub> atmosphere and 24 h.

<sup>a</sup>The Suzuki reactions of aryl halide with arylboronic acid catalyzed by Pd-CUs/LDH catalysts.

<sup>b</sup>The Suzuki reactions of aryl halide with arylboronic acid catalyzed by Pd-TROCs/LDH catalysts.

<sup>c</sup>The Suzuki reactions of aryl halide with arylboronic acid catalyzed by Pd-TRPLs/LDH catalysts.

<sup>d</sup>GC yield.

## 6. Mercury poisoning test

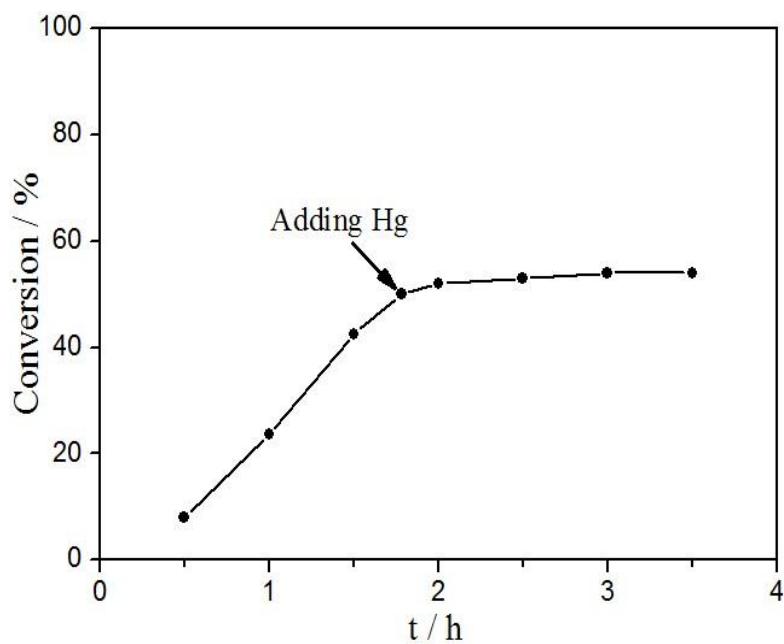


**Figure S3.** The mercury poisoning test of the Pd-CUs/LDH catalysts in Suzuki reaction of phenylboronic acid and iodobenzene.

## 7. TEM image of the spent Pd-CUs/LDH catalyst

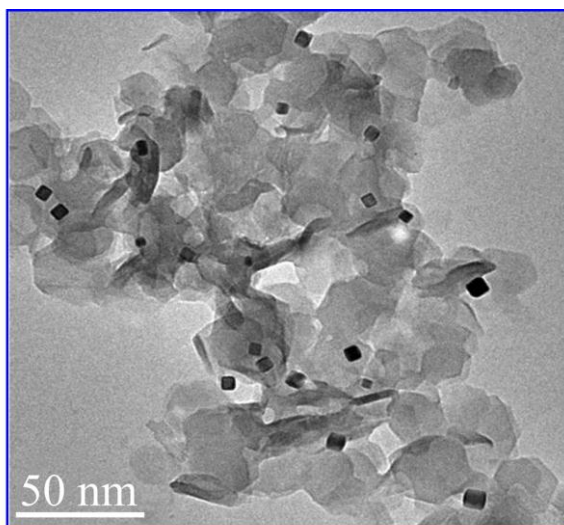


**Figure S4.** The TEM image of Pd-CUs/LDH catalyst after four catalytic cycles confirms that the

morphology of Pd nanocubes can be well maintained.

## 8. X-ray Photoelectron Spectroscopy (XPS) analysis

The solution containing the as-prepared Pd-CUs/LDH catalysts (80 mg), bromobenzene (1 mmol),  $K_2CO_3$  (2.4 mmol, 332 mg) and 10 mL of ethanol/water (4 : 1 volume ratio) solvent was added into a 100-mL, three-neck flask and stirred at 75 °C for 10 h under nitrogen atmosphere. The recovered catalysts were designated as sample 1; the preparation of sample 2 was similar to that for sample 1, except that phenylboronic acid (1.2 mmol) was also added into the mixed solution. The pristine Pd-CUs/LDH catalysts, sample 1 and 2 were characterized by XPS.

The XPS spectra of Pd-CUs/LDH catalysts shows the binding energy (BE) peaks of  $Pd^0$   $3d_{5/2}$  and  $3d_{3/2}$  at 335.1 and 340.4 eV, respectively (Figure S4A). Furthermore, the  $Pd^{2+}$  peaks (BE = 336.7 and 341.6 eV) can be observed. Considering the  $3d_{5/2}$  peak of  $Pd^{2+}$  in the  $K_2PdCl_4$  is located at 337.9 eV, the possibility of the  $PdCl_4^{2-}$  adsorbed on LDH sheet is excluded; here the  $Pd^{2+}$  peaks can be assigned to PdO at the surface of Pd NCs due to its exposure to an oxygen-containing environment.<sup>3</sup> For sample 1 and 2, besides of the BE peaks of Pd  $3d_{5/2}$  and  $3d_{3/2}$  for  $Pd^0$  and PdO, the XPS of Pd  $3d_{5/2}$  and  $3d_{3/2}$  shows new peaks at 336.4, 342.1 and 336.5, 342.0 eV respectively (Figure S5B, C), which can be attributed to the formation of organopalladium intermediate such as Ph-Pd-Br and/or Ph-Pd-B(OH)<sub>3</sub><sup>-</sup> during the catalytic reactions.<sup>1,4</sup> The BE peaks of I  $3d_{5/2}$  and  $3d_{3/2}$  at 618.4 and 631.2 eV respectively can also be observed (Figure S5D, inset), which can be attributed to the existence of I<sup>-</sup> ions on the surface of Pd NCs by chemical absorption. Here we acknowledge that the halide ions adsorbed on the surface of Pd NCs may have a potential influence on the catalysts. Due to the limitation of experimental conditions, however, we ignore the influence of chemically adsorbed halide ions on the Pd-NCs/LDH catalysts, and primarily focus on the role of

Pd-NCs/LDH catalysts with different morphologies and exposed facets for Pd NCs in the catalytic performances of Suzuki cross-coupling reactions. The plausible heterogeneous reaction mechanism can be put forward, where the Pd nanocubes surface undergoes oxidative addition with Ph-Br and Ph-B(OH)<sub>3</sub><sup>-</sup> to form Ph-Pd-Br and Ph-Pd-B(OH)<sub>3</sub><sup>-</sup> as possible transition states, which is similar to the reaction pathways described for the homogeneous catalysts.

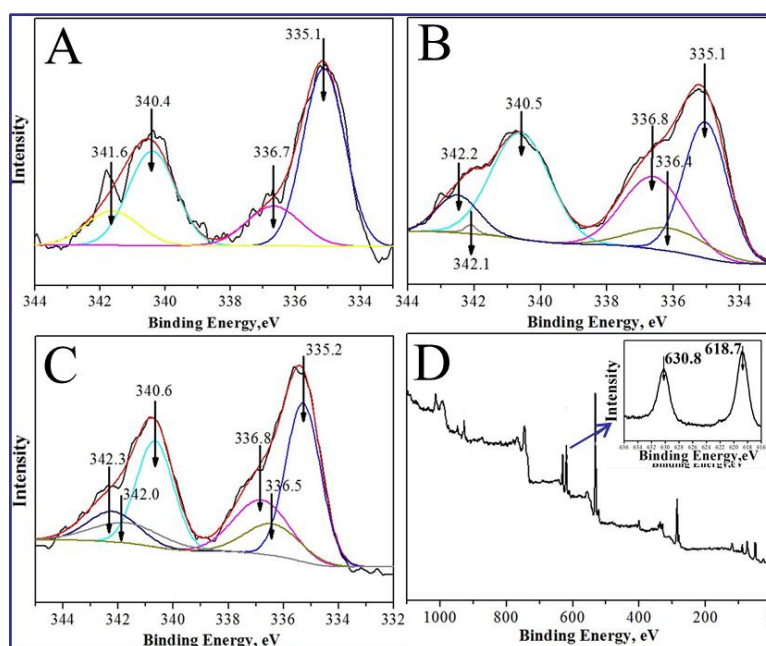


**Figure S5.** Pd 3d XPS spectra of the samples: (A) pristine Pd-CUs/LDH, (B) sample 1 and (C) sample 2. (D) XPS survey scan of pristine Pd-CUs/LDH along with I 3d<sub>5/2</sub> and 3d<sub>3/2</sub> (chemically adsorbed I<sup>-</sup> ions).

#### References:

- (1) B. M. Choudary, S. Madhi, N. S. Chowdari, M. L. Kantam and B. Sreedhar, *J. Am. Chem. Soc.*, 2002, **124**, 14127.
- (2) (a) X. Xiang, H. I. Hima, H. Wang and F. Li, *Chem. Mater.*, 2008, **20**, 1173; (b) S. D. Li, J. Lu, J. Xu, S. L. Dang, D. G. Evans and X. Duan, *J. Mater. Chem.*, 2010, **20**, 9718.
- (3) (a) E. H. Voogt, A. J. M. Mens, O. L. J. Gijzeman and J. W. Gens, *Surf. Sci.*, 1996, **350**, 21; (b) G. R. Cairns, R. J. Cross and D. Stirling, *J. Mol. Catal. A: Chem.*, 2001, **172**, 207; (c) F. Wang and

G. X. Lu, *J. Phys. Chem. C.*, 2009, **113**, 17070.

(4) (a) B. M. Choudary, S. Madhi, M. L. Kantam, B. Sreedhar and Y. Iwasawa, *J. Am. Chem. Soc.*, 2004, **126**, 2292; (b) E. Negishi, T. Takahashi, S. Baba, D. E. van Horn and N. Okukado *J. Am. Chem. Soc.*, 1987, **109**, 2393.